



**University of  
Zurich<sup>UZH</sup>**

**Zurich Open Repository and  
Archive**

University of Zurich  
University Library  
Strickhofstrasse 39  
CH-8057 Zurich  
[www.zora.uzh.ch](http://www.zora.uzh.ch)

---

Year: 2018

---

## **Sensitivity of intervertebral joint forces to center of rotation location and trends along its migration path**

Senteler, Marco ; Aiyangar, Ameet ; Weisse, Bernhard ; Farshad, Mazda ; Snedeker, Jess G

**Abstract:** Translational vertebral motion during functional tasks manifests itself in dynamic loci for center of rotation (COR). A shift of COR affects moment arms of muscles and ligaments; consequently, muscle and joint forces are altered. Based on posture- and level-specific trends of COR migration revealed by in vivo dynamic radiography during functional activities, it was postulated that the instantaneous COR location for a particular joint is optimized in order to minimize the joint reaction forces. A musculoskeletal multi-body model was employed to investigate the hypotheses that (1) a posterior COR in upright standing and (2) an anterior COR in forward flexed posture leads to optimized lumbar joint loads. Moreover, it was hypothesized that (3) lower lumbar levels benefit from a more superiorly located COR. The COR in the model was varied from its initial position in posterior-anterior and inferior-superior direction up to  $\pm 6$  mm in steps of 2 mm. Movement from upright standing to 45° forward bending and backwards was simulated for all configurations. Joint reaction forces were computed at levels L2/L3 to L5/S1. Results clearly confirmed hypotheses (1) and (2) and provided evidence for the validity of hypothesis (3), hence offering a biomechanical rationale behind the migration paths of CORs observed during functional flexion/extension movement. Average sensitivity of joint force magnitudes to an anterior shift of COR was +6 N/mm in upright and -21 N/mm in 30° forward flexed posture, while sensitivity to a superior shift in upright standing was +7 N/mm and -8 N/mm in 30° flexion. The relation between COR loci and joint loading in upright and flexed postures could be mainly attributed to altered muscle moment arms and consequences on muscle exertion. These findings are considered relevant for the interpretation of COR migration data, the development of numerical models, and could have an implication on clinical diagnosis and treatment or the development of spinal implants.

DOI: <https://doi.org/10.1016/j.jbiomech.2017.10.027>

Posted at the Zurich Open Repository and Archive, University of Zurich

ZORA URL: <https://doi.org/10.5167/uzh-142922>

Journal Article

Originally published at:

Senteler, Marco; Aiyangar, Ameet; Weisse, Bernhard; Farshad, Mazda; Snedeker, Jess G (2018). Sensitivity of intervertebral joint forces to center of rotation location and trends along its migration path. *Journal of Biomechanics*, 70:140-148.

DOI: <https://doi.org/10.1016/j.jbiomech.2017.10.027>



Contents lists available at ScienceDirect

Journal of Biomechanics

journal homepage: [www.elsevier.com/locate/jbiomech](http://www.elsevier.com/locate/jbiomech)  
[www.JBiomech.com](http://www.JBiomech.com)

# Sensitivity of intervertebral joint forces to center of rotation location and trends along its migration path

Marco Senteler<sup>a,b,c,1</sup>, Ameet Aiyangar<sup>c,1</sup>, Bernhard Weisse<sup>c</sup>, Mazda Farshad<sup>a</sup>, Jess G. Snedeker<sup>a,b,\*</sup>

<sup>a</sup> Department of Orthopedics, Balgrist Hospital, University of Zurich, Switzerland

<sup>b</sup> Institute for Biomechanics, ETH Zurich, Switzerland

<sup>c</sup> Empa, Swiss Federal Laboratories for Materials Science and Technology, Dübendorf, Switzerland

## ARTICLE INFO

### Article history:

Accepted 27 October 2017

Available online xxxxx

### Keywords:

Lumbar spine

Center of rotation

Musculoskeletal model

Inverse dynamic musculoskeletal analysis

Intervertebral joint loading

Muscle moment arm

## ABSTRACT

Translational vertebral motion during functional tasks manifests itself in dynamic loci for center of rotation (COR). A shift of COR affects moment arms of muscles and ligaments; consequently, muscle and joint forces are altered. Based on posture- and level-specific trends of COR migration revealed by in vivo dynamic radiography during functional activities, it was postulated that the instantaneous COR location for a particular joint is optimized in order to minimize the joint reaction forces. A musculoskeletal multi-body model was employed to investigate the hypotheses that (1) a posterior COR in upright standing and (2) an anterior COR in forward flexed posture leads to optimized lumbar joint loads. Moreover, it was hypothesized that (3) lower lumbar levels benefit from a more superiorly located COR.

The COR in the model was varied from its initial position in posterior-anterior and inferior-superior direction up to  $\pm 6$  mm in steps of 2 mm. Movement from upright standing to 45° forward bending and backwards was simulated for all configurations. Joint reaction forces were computed at levels L2/L3 to L5/S1. Results clearly confirmed hypotheses (1) and (2) and provided evidence for the validity of hypothesis (3), hence offering a biomechanical rationale behind the migration paths of CORs observed during functional flexion/extension movement. Average sensitivity of joint force magnitudes to an anterior shift of COR was +6 N/mm in upright and −21 N/mm in 30° forward flexed posture, while sensitivity to a superior shift in upright standing was +7 N/mm and −8 N/mm in 30° flexion. The relation between COR loci and joint loading in upright and flexed postures could be mainly attributed to altered muscle moment arms and consequences on muscle exertion. These findings are considered relevant for the interpretation of COR migration data, the development of numerical models, and could have an implication on clinical diagnosis and treatment or the development of spinal implants.

© 2017 Elsevier Ltd. All rights reserved.

## 1. Introduction

Given the infeasibility of directly and non-invasively measuring forces within the lumbar spine in vivo, they are usually inferred from kinematics-driven biomechanical models such as *linked segment*-, *finite element*- or *multi-body models* (Abouhossein et al., 2011; Cholewicki et al., 1991; Christophy et al., 2012; Daggfeldt and Thorstensson, 2003; De Zee et al., 2007; Han et al., 2013b; Schultz et al., 1982). Since biomechanical model output is highly sensitive to kinematic inputs, a high degree of accuracy in the kinematic input is particularly imperative. One key kinematic input

parameter is the definition of a so-called center of rotation (COR) between intervertebral segments around which relative segment motion can be described in terms of rotation around this center in anatomical three planes.

Several studies have shown that lumbar segments exhibit coupled translations associated with rotational movement. Mapping the migration path of the instantaneous centers of rotation (ICRs) between two adjacent vertebrae over a given motion – the centrode – has been shown to be a reasonable way to quantitatively describe such coupled motion (Aiyangar et al., 2017; Gertzbein et al., 1984; Ogston et al., 1986). More importantly, the ICR have been shown to have a biological basis linking aberrations in its location to anatomical and pathological factors (Bogduk et al., 1995; Schneider et al., 2005), based on its strong association with the center of reaction (Gracovetsky et al., 1987; Zander et al., 2016). Despite this evidence, a fixed center three-degree-of-

\* Corresponding author at: University Hospital Balgrist, Lengghalde 5, 8008 Zurich, Switzerland.

E-mail address: [snedeker@ethz.ch](mailto:snedeker@ethz.ch) (J.G. Snedeker).

<sup>1</sup> Shared first authorship.

freedom (DOF) rotational joint with a fixed COR that approximates an average location has been the *choice de rigueur* for representing the intervertebral disc joint (Bruno et al., 2015a; Christophy et al., 2012; De Zee et al., 2007). This compromise in using an averaged, fixed COR in biomechanical models is often forced by a lack of robust data from which migration patterns of the instantaneous centers of rotation can be extracted (De Zee et al., 2007). This shortcoming can be at least attributed to the according lack of accurate means to map these patterns during spinal movement (Crisco et al., 1994; Percy and Bogduk, 1988) and partly due to a lack of quantification of the biomechanical implications of simplifying a 6 DOF motion into a purely rotational one. Small changes in the presumed location of the COR and, by association, the centers of reaction (Bogduk et al., 1995; Gracovetsky et al., 1987; Schneider et al., 2005; Zander et al., 2016), can sufficiently alter estimates of muscle and ligament moment arms such as to provoke significant variations in the corresponding estimates of generated muscle force (Han et al., 2013a; Zander et al., 2016; Zhu et al., 2013). These variations in turn strongly influence estimation of net joint forces and moments, and joint reaction forces (Zander et al., 2016). Secondly, since loads in the spine are shared between the anterior components—vertebral body and intervertebral disc—and the posterior elements—the facet joint complex—, uncertainties in force estimations within the disc can lead to inaccuracies in the estimation of loads within the segment facet joints as well as the adjacent segments (Dooris et al., 2001; Han et al., 2013a; Zander et al., 2009). However, the current literature does not provide robust explanations for the observed dynamics of center of rotation during functional tasks, particularly in a manner that enables reasonable prediction of COR trajectory during a specific movement.

The longstanding limitations regarding lacking data is being overcome with recent developments in direct measurement of bone kinematics using dynamic radiographic techniques, particularly during in vivo load bearing functional activities (Ahmadi et al., 2009; Aiyangar et al., 2014; Anderst et al., 2008; Wu et al., 2014). Very recently, Aiyangar et al. mapped the migration patterns of the instantaneous COR during a lifting task using dynamic stereo radiography (DSX) to show that the COR generally migrates from an anterior-most location towards a posterior location during a progressive extension movement from a forward flexed to an upright position (Aiyangar et al., 2017). Further they also demonstrated that the average COR superior-inferior (SI) location is level-specific, with the average SI coordinates tending to be located in an increasingly superior location as one moves inferiorly from L2/L3 toward the lowest anatomical segment (L5/S1).

Given these recent insights into COR migration patterns during specific functional lifting activity, we postulated that the instantaneous COR location for a specific joint is optimized to minimize the joint reaction forces within the intervertebral disc of that particular joint. We designed the current study to test the following hypotheses:

1. In a flexed position, an anterior location of COR results in the lowest magnitude joint reaction force.
2. In an upright position, a posteriorly located COR results in lowest magnitude joint reaction force.
3. In inferior lumbar segments the lowest joint reaction forces result from more superior locations of COR as compared to upper segments.

## 2. Methods

The effect of COR location on joint reaction forces was investigated using a recently described and publicly available kinematics driven upper body musculoskeletal model (Senteler et al., 2016) for

OpenSim® (Delp et al., 2007). The model represents a generic human male with a height of 170 cm and 71 kg body weight. It includes the body segments from the femur bones upwards. The lumbar spine is implemented using six body segments from the first lumbar level to the sacrum. The pelvis and sacrum are treated as a single rigid construct, as is the thorax consisting of the thoracic vertebrae and ribcage. Additional bodies for cervical spine, head, upper and lower arms, and hands complement the model. Mass and inertia properties are assigned to all body segments based on the literature (Pearsall et al., 1996; Shan and Bohn, 2003). The geometric representation of bones were adopted from previous models (Christophy et al., 2012; Holzbaur et al., 2005; Vasavada et al., 1998). Each body within the model included its own coordinate system which could be selected as local reference frames to express simulation results such as joint forces or body kinematics. Vertebrae-specific coordinate system origins were located in the middle of the corresponding vertebral body's posterior edge as shown in Fig. 1. The x-axes are aligned with the bisector of upper and lower endplate. The muscle architecture and force generating capacity of individual muscles was directly adopted from the lumbar spine model of Christophy et al. (2012).

Muscle moment arms were obtained as outputs from the OpenSim (Delp et al., 2007) software. Briefly, muscle moment arms are defined in OpenSim as follows:

$$r_{\theta} = \frac{\tau_{\theta}}{s} \quad (1)$$

with the equivalent definition based on the “tendon-excision method” as:

$$r_{\theta} = \frac{dl}{d\theta} \quad (2)$$

where

$r_{\theta}$  = muscle moment arm specific to a joint-associated kinematic quantity, “ $\theta$ ”

$\tau_{\theta}$  = scalar quantity representing the effective torque acting about “ $\theta$ ” due to the scalar tension force, “ $s$ ” generated by muscle activation.

$dl/d\theta$  = change in length ( $dl$ ) of the muscle effected by a small displacement ( $d\theta$ ).

The algorithm implemented in OpenSim version 3.0 and beyond uses a Generalized Force Method to directly satisfy the definition of moment arm according to Eq. (1) rather than the perturbation method to compute muscle moment arms based on the tendon excursion method. See (Sherman et al., 2013) for further details.

The model included joint bushings for each of the lumbar levels, with assigned stiffness being individually calibrated based on load controlled *in vitro* experiments to account for influence of the intervertebral disc as well as passive elements such as ligaments and joint capsules. In a neutral position of the lumbar spine represented by upright standing, the bushing forces were zero. All details on model implementation and extensive corroboration of model predictions against joint reaction forces from the literature are described elsewhere (Senteler et al., 2014, 2016, 2017).

To investigate the effects of COR on generated joint forces, a sinusoidal lumbar extension motion from 45° forward flexed posture to upright standing was simulated. Motion was restricted to the sagittal plane and did not include vertebral translations; pure rotation was simulated around the fixed COR of each vertebra. Rotational range of motion was distributed among vertebral levels as described in the original lumbar spine model (Christophy et al., 2012; Senteler et al., 2016). A static optimization algorithm minimizing squared muscle activation (OpenSim default) was employed to predict the muscle forces best matching the

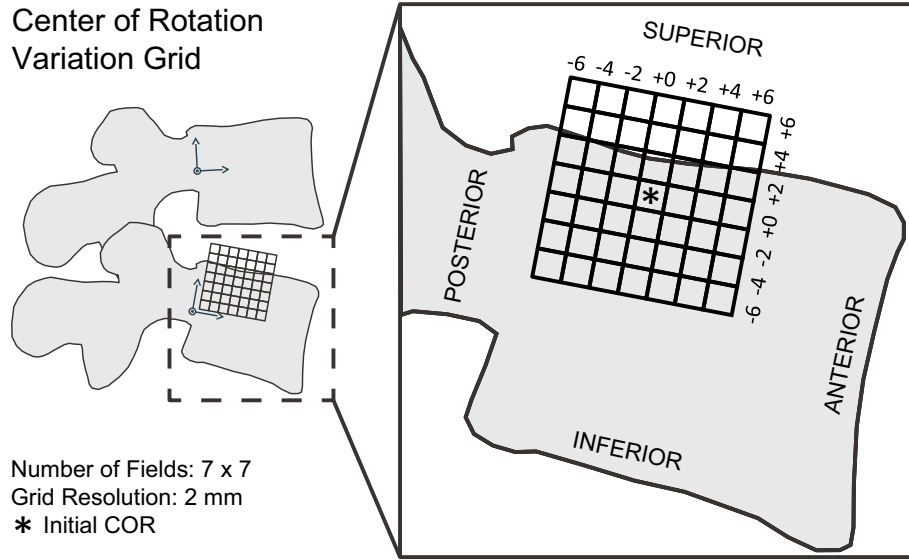


**Fig. 1.** Motion segment with COR variation grid projected on right sagittal section view. The initial COR as defined by Christophy et al. (2012) according to Wong et al. (2006) is located at grid coordinates +0/+0 as illustrated by asterisk (\*).

pre-defined kinematics. Initial COR positions were adopted from those used in the previously published upper body model (Senteler et al., 2016) as based on locations reported in the work of Percy and Bogduk (1988). CORs were then adjusted simultaneously and equally at all levels, systematically in up to 3 steps of 2 mm in combined posterior-anterior (PA) and SI direction (maximal  $\pm 6$  mm, 49 combinations in total). Level-specific definitions of AP and SI direction corresponded with the inferior vertebra's local coordinate system. The covered range of COR variation approximately represents 50% of the vertebral body size and is in accordance with physiological COR migration distances during extension movement as measured in in vivo kinematic assessments (Aiyangar et al., 2017). To avoid bushing forces caused by the translation of CORs the joint bushings were repositioned to match with the new joint centers. Initial muscle lengths remained unchanged throughout all configurations; hence no scaling of muscle properties was required after changing COR.

Variations of COR resulted in a total of 49 ( $7 \times 7$ ) configurations, represented by the COR variation grid (Fig. 1); a single simulation was performed for each configuration. Assigning results of each simulation to the corresponding field of the COR variation grid led to a  $7 \times 7$  force matrix (Eq. (3)) with increasing row- and column indices standing for increasingly inferior and anterior COR locations, respectively. The matrix was thus specific for each spinal level and a selected posture (flexion angle). The center position of the matrix represents the initial standard COR configuration (0/0) of the model.

$$F(\text{level}, \text{flexion angle}) = \begin{bmatrix} F_{1,1} & \cdots & F_{1,7} \\ \vdots & & \vdots \\ F_{7,1} & \cdots & F_{7,7} \end{bmatrix} \quad (3)$$

In order to analyze the effect of a shift of COR on joint forces, the difference in force between the current COR and its neighboring COR positions was computed. Each COR location had neighbors in the PA and SI directions, providing two values per field that could be combined in a vector indicating the direction in which a COR shift increased joint force (Eq. (4)):

$$\mathbf{f}_{ij} = \begin{pmatrix} \Delta F_x \\ \Delta F_y \end{pmatrix} = \begin{pmatrix} F_{i,j+1} - F_{i,j} \\ F_{i+1,j} - F_{i,j} \end{pmatrix} \quad |i, j = 1, \dots, 6 \quad (4)$$

Normalizing this vector by grid resolution of 2 mm yielded a *gradient of joint force* at one particular COR location (Eq. (5)), whose dimension was N/mm.

$$\mathbf{g}_{ij} = \frac{1}{2 \text{ mm}} \cdot \mathbf{f}_{ij} \quad |i, j = 1, \dots, 6 \quad (5)$$

An *average joint reaction force gradient* throughout the variation grid was then calculated as a general measure of tendency for effects due to shifts of COR in either direction (Eq. (6)), together with its 95% confidence interval. The average gradient is specific for a selected force component at one spinal level in a particular posture.

$$\mathbf{g}_{avg} = \begin{pmatrix} g_{avg,PA} \\ g_{avg,SI} \end{pmatrix} = \frac{1}{42} \cdot \sum_i \sum_j \mathbf{g}_{ij} \quad (6)$$

All simulation data analysis was performed in MATLAB (R2012b, The MathWorks Co. Ltd.).

### 3. Results

Simulations clearly indicated joint reaction force sensitivity to the imposed location of joint COR (Tables 1 and 2). Total muscle forces per muscle group as computed for the initial COR configuration (0/0) in the upright standing and 45° flexed posture are summarized in Fig. 3. Maximum absolute and relative deviations of computed joint forces from reference values after CORs were modified within the range of the grid ( $\pm 6$  mm in PA and SI direction) for each intervertebral level (L2 to S1) and selected degrees of forward flexion (0°, 15°, 30°, 45°; Table 2). Fig. 2 contains a visual representation of results for the upright standing and 45° forward flexed posture in each of the 49 COR configurations. In general, larger gradients are found for the flexed than for the upright posture. Increasing spread of values with progressing flexion angles was observed at all levels, with compression forces more affected at lower levels and shear forces at upper levels. *Compression forces* were clearly the dominant force component of *total joint forces* thus very similar in quality and quantity to total joint forces. Magnitudes of maximum force increase and force decrease over simulated CORs were similar for the upright posture, whereas in flexed postures a tendency for force increases were more prevalent.

**Table 1**  
Joint reaction force values computed during simulation of sinusoidal extension motion from 45° forward flexed to upright standing (0°) using the initial COR location (+0/+0): (a) compression, (b) shear, (c) total force.

	0°	15°	30°	45°
<i>(a) Compression Forces [N]</i>				
L2L3	464	537	795	1089
L3L4	463	528	784	1107
L4L5	527	577	846	1191
L5S1	517	569	834	1178
<i>(b) Posterior-Anterior Shear Forces [N]</i>				
L2L3	−42	−15	22	94
L3L4	49	52	84	136
L4L5	164	161	230	307
L5S1	249	226	291	342
<i>(c) Resultant Total Forces [N]</i>				
L2L3	466	538	796	1093
L3L4	465	530	788	1115
L4L5	551	599	877	1230
L5S1	573	612	883	1227

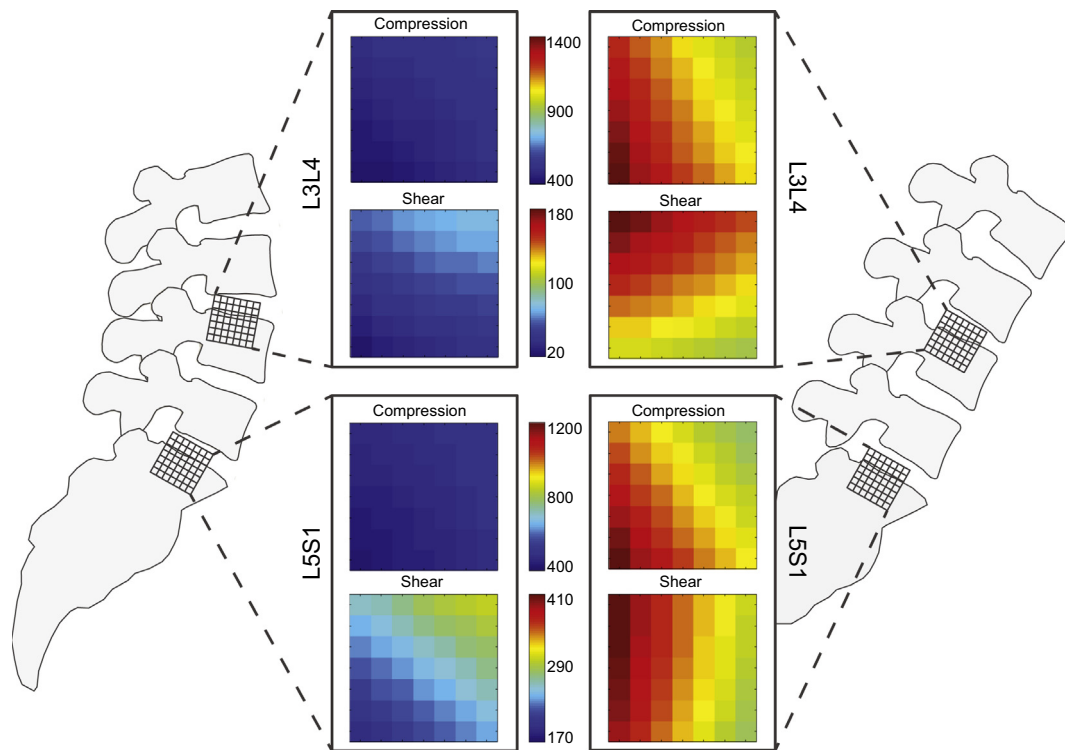


**Fig. 2.** Map plots visualizing compression and shear force magnitude for all simulated CORs ( $7 \times 7$  grid) at levels L3L4 (top) and L5S1 (bottom) for upright standing (left) and 45° forward flexed posture (right). Note that the COR locations were changed at all level simultaneously and to the same extent, which means that results of one simulation are reflected at all levels in the same field (i.e. the results for the 0/0 initial configuration for all levels was obtained by the joint force computation in the initial model configuration).

Average relative joint reaction force gradients of shear and compression forces (force change in % per mm of COR shift) are shown in Fig. 4. Posterior locations of COR were generally associated with lower forces in the upright position. A more anterior COR in the upright position increased compression forces at all levels, between +5.4 and +5.8 N/mm on average (+1.0%/mm to +1.3%/mm). Shear forces also increased, between +1.3 and +4.0 N/mm from L3 to S1 (+1.6%/mm to +2.7%/mm); only at level L2L3 an anterior COR slightly decreased shear forces (−0.2 N or −0.5%/mm). In contrast, in a 30° forward flexed posture more anterior CORs lowered compression and shear at all levels between −19.7 N/mm and −21.7 N/mm (−2.5%/mm to −2.7%/mm) and −0.1 N/mm to −7.3 N/mm (−0.6%/mm to −2.5%/mm), respectively. Compression force

gradients in anterior direction were very similar at all spinal levels, with differences between the largest and smallest value of around 10% or less. In contrast, compression gradients in superior direction differed substantially between upper and lower levels, particularly in forward flexed postures (30°, 45°): A more superior COR at L4L5 and L5S1 reduced the resulting compression forces by around 50% more than at upper levels for the same amount of COR displacement.

Shear force gradients in both directions varied remarkably between vertebral levels. An anterior shift of COR did not much affect forces at levels L2L3 and L3L4 (between +1.3 N/mm and −2.2 N/mm). At lower levels on the other hand, absolute gradients ranged from +4 N/mm in upright standing to −8.7 N/mm in



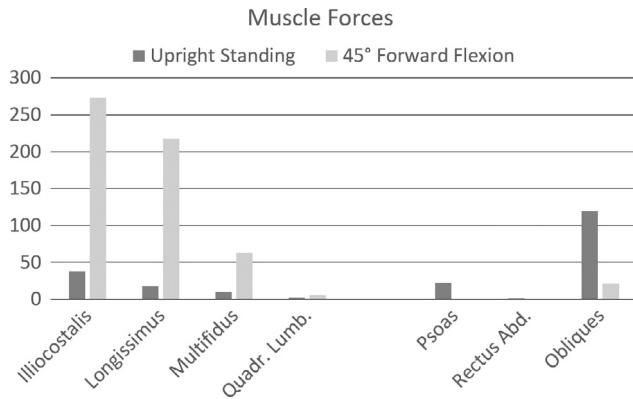


**Fig. 3.** Sum of muscle forces for the main muscle groups as computed for the initial model configuration (COR at 0/0 grid position) in the upright standing and 45° forward flexed posture.

forward flexion, again clearly indicating lower joint forces for posterior COR in upright and anterior COR in flexed postures. Shifting COR superiorly generally increased shear forces. Highest absolute gradients in upright standing were achieved at lower levels, whereas upper levels yielded the strongest absolute force gradients in flexion. If values were normalized by joint force magnitude, the sensitivity to SI location of COR seems to diminish from upper to lower segments.

Muscle moment arm analysis for the main extensor (*iliocostalis*, *lattissimus*) and flexor (*rectus abdominus*, *obliques*) muscle groups in the upright standing posture (Fig. 5) showed an average 23% increase and 22% decrease with respect to the neutral COR location, respectively. A COR at the posterior end of the variation grid reduced main extensor moment arms by 21% and increased those of flexor muscles by 20%. In contrast, moving the COR inferiorly or superiorly altered average moment arms by only −1% to +3%,

respectively. Generally, moment arms were nearly identically affected in upright as in flexed postures.

#### 4. Discussion

The concept of migrating CORs, along with its potential utility in diagnosing different pathological conditions of the lumbar spine has long been discussed (Gertzbein et al., 1986, 1985; Ogston et al., 1986). However, large precision errors associated with available measurement techniques has precluded practical use of this phenomenon (Crisco et al., 1994; Percy and Bogduk, 1988). Settling for an average COR was then considered the best approach to minimizing errors when representing the rotational kinematics within the lumbar joints (Percy and Bogduk, 1988). Indeed, representing lumbar joints as rotational joints with a fixed COR is almost universally applied (Daggfeldt and Thorstensson, 2003; De Zee et al., 2007; Delp et al., 2007; Senteler et al., 2016; Zhu et al., 2013) and is one of the basic design aspects featured in modern prosthetic disc replacements (Dreischarf et al., 2015). Recent improvements in dynamic imaging techniques (Ahmadi et al., 2009; Aiyangar et al., 2014; Anderst et al., 2008; Wu et al., 2014), and the ability to compute instantaneous axes of rotation for smaller rotational step sizes (Aiyangar et al., 2017; Baillargeon and Anderst, 2013; Ellingson and Nuckley, 2015), however, has rekindled interest in utilizing instantaneous COR patterns for identifying pathologies such as lumbar instability (Ahmadi et al., 2009) and degenerative spondylolisthesis (Ellingson and Nuckley, 2015). At the same time, Zander and co-workers demonstrated the inaccuracy of the accepted “average” COR in locating the point where muscle activity and joint reaction forces are minimized for a static upright pose, using the center of reaction concept (Zander et al., 2016).

The current simulation study supports and elaborates earlier modelling studies (Dooris et al., 2001; Han et al., 2013a; Zander et al., 2016; Zhu et al., 2013) that critically examined the

**Table 2**

Maximum positive and negative deviations of joint reaction forces after COR modification in PA and SI directions (along a grid of 7 × 7 fields with 2 mm spacing; see also Fig. 1). Absolute differences in [N] and relative differences in [%] with respect to the forces computed for the initial COR position (100%).

	0°	15°	30°	45°
<i>(a) Maximum Deviations of Compression Forces ([N] and [%])</i>				
L2L3	+78/−76 N +17/−16%	+109/−87 N +20/−16%	+191/−122 N +24/−15%	+274/−179 N +25/−16%
L3L4	+68/−71 N +15/−15%	+90/−74 N +17/−14%	+195/−120 N +25/−15%	+286/−189 N +26/−17%
L4L5	+60/−63 N +11/−12%	+115/−70 N +20/−12%	+253/−143 N +30/−17%	+362/−231 N +30/−19%
L5S1	+53/−55 N +10/−11%	+110/−64 N +19/−11%	+244/−138 N +29/−16%	+354/−225 N +30/−19%
<i>(b) Maximum Deviations of Posterior–Anterior Shear Forces ([N] and [%])</i>				
L2L3	+13/−10 N +32/−23%	+18/−15 N +120/−126%	+29/−26 N +134/−119%	+45/−36 N +48/−38%
L3L4	+22/−10 N +46/−56%	+26/−17 N +51/−33%	+36/−21 N +42/−25%	+44/−36 N +32/−27%
L4L5	+45/−45 N +28/−27%	+44/−33 N +27/−20%	+53/−36 N +23/−16%	+67/−57 N +22/−18%
L5S1	+54/−53 N +22/−21%	+51/−39 N +23/−17%	+55/−37 N +19/−13%	+66/−57 N +19/−17%
<i>(c) Maximum Deviations of Resultant Total Forces ([N] and [%])</i>				
L2L3	+77/−74 N +17/−16%	+108/−86 N +20/−16%	+191/−121 N +24/−15%	+271/−176 N +25/−16%
L3L4	+71/−73 N +15/−16%	+93/−75 N +17/−14%	+193/−119 N +25/−15%	+282/−187 N +25/−17%
L4L5	+71/−73 N +13/−13%	+114/−76 N +19/−13%	+254/−145 N +29/−16%	+360/−231 N +29/−19%
L5S1	+72/−72 N +13/−13%	+110/−74 N +18/−12%	+247/−141 N +28/−16%	+354/−227 N +29/−18%

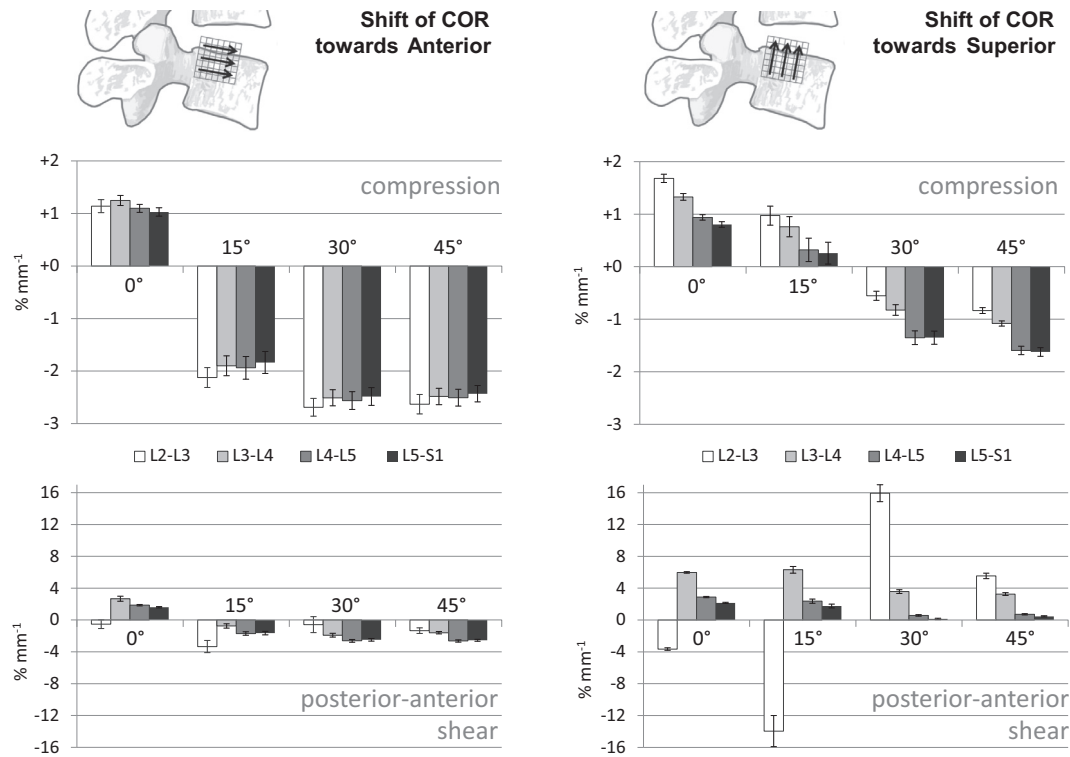


**Fig. 4.** Analysis of sensitivity of joint forces to COR migration in posterior-anterior (left hand side) and inferior-superior direction (right hand side). The upper graph represents sensitivity of compression forces, whereas the lower graph contains results for shear components. The sensitivity is provided as a relative change of joint forces per mm of COR displacement, and is visually represented by vertical bars; error bars indicate 95% confidence intervals. A positive value means that a shift of COR in the corresponding direction causes increase in loads, whereas a negative value designates joint force reduction. Sensitivity is normalized with respect to reported forces in the initial COR position, hence large percentage numbers may result in the case of shear forces, which are not necessarily appropriately reflecting the proportions of effects. Results are provided separately for distinct intervertebral levels (L23 to L5S1, according to bar shading) and four different poses (upright standing, 15°, 30°, and 45° forward flexion, reflected by bar grouping).

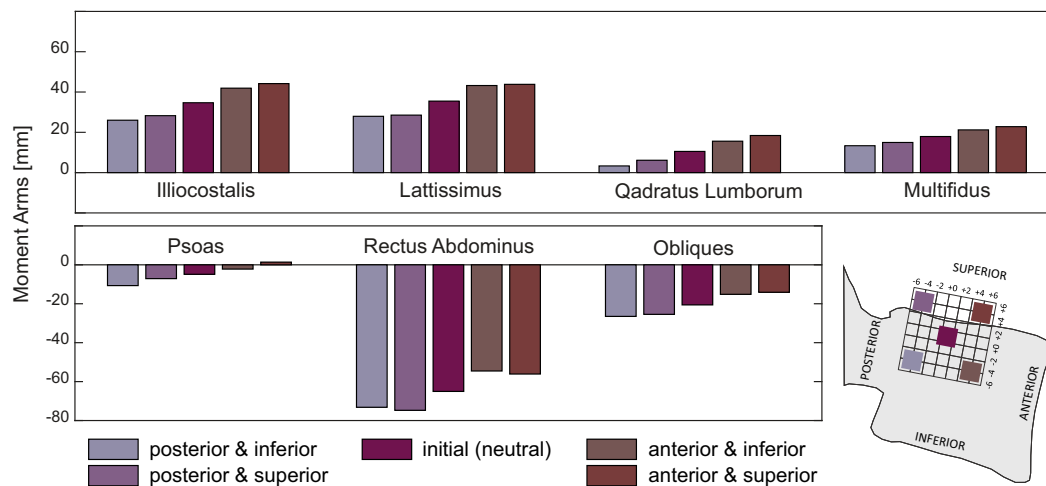


**Fig. 5.** Muscle moment arms in relation to COR location for selected extensor (top) and flexor muscle groups (bottom), as reported by OpenSim in the upright standing posture. A difference between maximally anterior and posterior COR locations is clearly apparent, while SI variation of COR has a relatively smaller effect.

appropriateness of assuming a fixed COR used for lumbar segments. The present work attempted to clarify the biomechanical basis underpinning the oft-cited observation of migrating CORs during lumbar intervertebral motion. Specifically we sought to test whether COR migration could serve as a primary mechanism for minimizing joint reaction forces at the intervertebral discs. To test this hypothesis, we estimated lumbar IVD forces using a kinematics driven musculoskeletal model that was recently developed and

validated for examining the joint level lumbar spine biomechanics (Senteler et al., 2016). The model estimates are in reasonably good agreement with reported forces in other, more recently published studies (Arjmand et al., 2011; Han et al., 2013a; Ignasiak et al., 2015).

The hypothesis of the present study that COR migration during functional flexion-extension tasks follows a trajectory that minimizes joint reaction forces within the intervertebral joints was

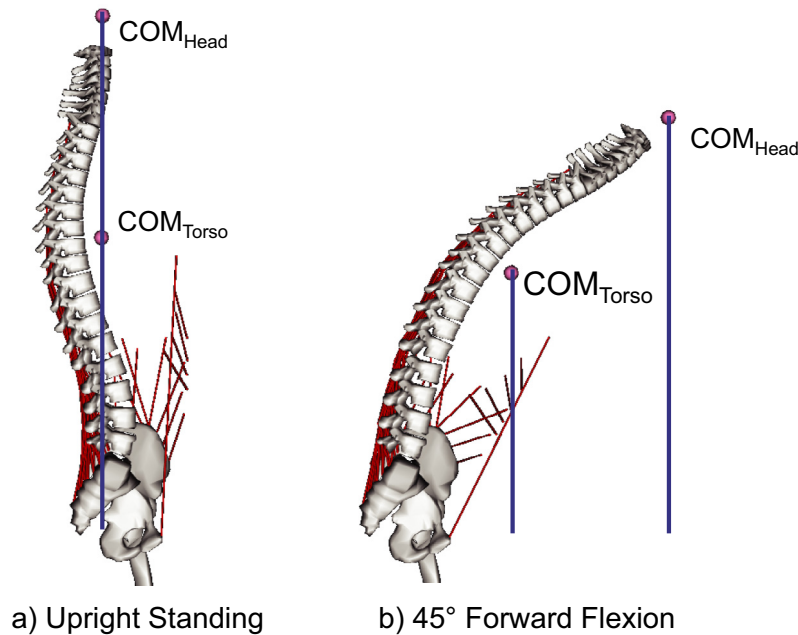


**Fig. 6.** Center of mass locations of head and torso in upright standing (a) and 45° forward flexed posture. In upright posture mass lever arms are comparably small as opposed to the flexed posture, explaining high extensor muscle activity in forward flexion and during lifting.

supported by the model predictions. Specifically, the study corroborated previous conjecture based on experimental observations of lumbar segmental kinematics (Aiyangar et al., 2017):

1. In forward flexed positions an anterior location of COR is favorable at all spinal levels, as indicated by negative compression and shear force gradients towards more anteriorly located CORs in all flexed postures (Figs. 2 and 4).
2. In an upright position, joint reaction force minimization requires relatively posteriorly located CORs, as indicated by positive compression and shear force gradients in anterior direction (Figs. 2 and 4).

The study also demonstrated differences between upper and lower levels, with reduction in joint force per unit of COR migration in AP direction being greater at the lower lumbar levels. To explain these effects on joint loads, altered muscle moment arms and muscle forces, as well as center of mass locations must be considered. In both an upright as well as flexed posture, an anterior COR decreases flexor and increases extensor muscle moment arms. In upright standing, the gravity line of cranial body segment masses falls slightly behind most lumbar CORs in the model (Fig. 6). Thus maintenance of posture requires activation of flexor muscles, with slightly larger forces required if their moment arms are reduced by an anterior COR. This effect dominates lowered extensor forces, since the latter are less active. Consequently, joint forces slightly increase. A flexed posture on the other hand requires significant extensor exertion to balance the body masses. Given the rather small moment arms of extensor muscles, an anterior COR causes a remarkable reduction of muscle forces. As most of the joint loads in flexed posture can be attributed to muscle forces, an anterior COR dramatically lowers joint loads in the whole range of forward flexion. This rationale not only provides a biomechanical explanation for the opposite effect of anterior COR migration in upright vs. flexion but also for more heavily affected joint loads in flexed postures.

Analyzing the influence of the superior-inferior location of the COR on joint reaction force was less straightforward. Simulations

of upright standing revealed increased compressive forces across all segments for more superior COR locations, as indicated by the positive force gradients, but the increases were more drastic for the upper segments (L2L3 = +1.7%/mm; L3L4 = 1.3%/mm) compared to the lower segments (L4L5 = +0.9%/mm; L5S1 = +0.8%/mm). This resulted in total variations between most inferior and most superior COR locations of +20%, +16%, +11% and +10% at levels L2L3, L3L4, L4L5 and L5S1 respectively. The opposite trend was observed in more flexed positions. Decreased compressive force levels were observed across all levels. Perhaps more importantly, force reductions were relatively smaller for the upper segments {L2L3 = -6% (-0.6%/mm) and -10% (-0.8%/mm); L3L4 = -10% (-0.8%/mm) and -13% (-1.1%/mm) for 30 and 45 degree of flexion, respectively} compared to the lower segments L4L5 and L5S1 {both -16% (-1.4%/mm) and -19% (-1.6%/mm) for 30 and 45 degree of flexion, respectively}. Averaging the results over all tested positions revealed an overall positive gradient for L2L3 (+0.3%/mm) while L5S1 showed an overall negative gradient (-0.5%/mm). Gradients for L3L4 (0.0%/mm) and L4L5 (-0.4%/mm) fell between the bounds defined by L2L3 and L5S1. These results indicate that, on average, a superiorly located COR might be more favorable for the lower segments (L4L5 and L5S1) while an inferiorly located COR is more favorable for the uppermost segment in terms of minimizing the forces experienced within the respective joint. This explanation is particularly justified since the load borne by the intervertebral joint during forward-flexed postures can approach safe loading limits of the lumbar spine (Arjmand et al., 2012; McGill, 1997), with a reduction of forces thus being more meaningful in that configuration. Although superiorly located CORs generally increased predicted shear forces at most levels, the force gain observed at lower levels in flexed postures was rather small. Hence, in conclusion, computational results at least partially affirm the third hypothesis underlying the current investigation; As the COR of a given segment moves superiorly towards the superior endplate of the inferior vertebra reaction forces are minimized at that joint.

We consider our findings to be highly relevant to the interpretation of COR migration data and the development of numerical



models. We nonetheless acknowledge that the findings of this work must be interpreted with caution, given the complex prevailing biomechanics of the lumbar spine. At the very least, the present work will help in clarifying results obtained with different spine modeling practices, particularly assumptions regarding the location of the COR, and, by association, the center of reaction.

Further, although the model simulations clearly demonstrate the plausibility of the concept that COR migration is a possible mechanism for minimizing joint reaction forces, the current study does not provide direct evidence. Alternative hypotheses and alternative approaches require investigation before accepting the basic premise of the current study. For example, recent studies pursuing a *force-dependent approach* (Arshad et al., 2017; Bruno et al., 2015b) to estimate kinematics that include the loci of CORs represent a valid alternative approach.

Further limitations include the fact that COR was restricted from migration (held constant) as each level was examined in parametric analysis (a  $7 \times 7$  grid for each level). However, this simplification was required to keep the scope of the analysis manageable, and allowed a visualization of COR migration based on reaction force mapping that would not be otherwise possible. Furthermore, the inertial effects of a moving COR were not necessarily accounted by the quasi-static optimization used at each simulation increment.

Also, the employed generic musculoskeletal model does not account for the anatomical, physiological and constitutional variations within the human population.

Finally, although range of COR migrations applied in our study was motivated by in vivo measurements, the amount was smaller than those used in other studies (Zander et al., 2016). Nevertheless, our results are considered complementary in that they clearly point out different trends for different postures (Fig. 2), and thus provide a physiologically meaningful explanation for the observed shift of COR during dynamic activities.

## Acknowledgement

The authors would like to acknowledge the Department of Orthopedics at the University of Zurich, and EMPA for funding of the study. We also acknowledge support received through the Ambizione Career Grant Award (PZ00P2\_154855/1) from the Swiss National Science Foundation (SNSF).

## Conflict of interest

The authors state that there is no conflict of interest to report.

## References

- Abouhossein, A., Weisse, B., Ferguson, S.J., 2011. A multibody modelling approach to determine load sharing between passive elements of the lumbar spine. *Comput. Methods Biomech. Biomed. Eng.* 14, 527–537.
- Ahmadi, A., Maroufi, N., Behtash, H., Zekavat, H., Parnianpour, M., 2009. Kinematic analysis of dynamic lumbar motion in patients with lumbar segmental instability using digital videofluoroscopy. *Eur. Spine J.* 18, 1677–1685.
- Aiyangar, A., Zheng, L., Anderst, W., Zhang, X., 2017. Instantaneous centers of rotation for lumbar segmental extension in vivo. *J. Biomech.* 52, 113–121.
- Aiyangar, A.K., Zheng, L., Tashman, S., Anderst, W.J., Zhang, X., 2014. Capturing three-dimensional in vivo lumbar intervertebral joint kinematics using dynamic stereo-X-ray imaging. *J. Biomech. Eng.* 136, 11004.
- Anderst, W.J., Vaidya, R., Tashman, S., 2008. A technique to measure three-dimensional in vivo rotation of fused and adjacent lumbar vertebrae. *Spine J.*
- Arjmand, N., Plamondon, A., Shirazi-Adl, A., Parnianpour, M., Larivière, C., 2012. Predictive equations for lumbar spine loads in load-dependent asymmetric one- and two-handed lifting activities. *Clin. Biomech.* 27, 537–544.
- Arjmand, N., Plamondon, A., Shirazi-Adl, A., Larivière, C., Parnianpour, M., 2011. Predictive equations to estimate spinal loads in symmetric lifting tasks. *J. Biomech.* 44, 84–91.
- Arshad, R., Zander, T., Bashkuev, M., Schmidt, H., 2017. Influence of spinal disc translational stiffness on the lumbar spinal loads, ligament forces and trunk muscle forces during upper body inclination. *Med. Eng. Phys.* 46, 54–62.
- Baillargeon, E., Anderst, W.J., 2013. Sensitivity, reliability and accuracy of the instant center of rotation calculation in the cervical spine during in vivo dynamic flexion-extension. *J. Biomech.* 46, 670–676.
- Bogduk, N., Amevo, B., Pearcy, M., 1995. A biological basis for instantaneous centres of rotation of the vertebral column. *Proc. Inst. Mech. Eng.* 209, 177–183.
- Bruno, A.G., Boussein, M.L., Anderson, D.E., 2015a. Development and validation of a musculoskeletal model of the fully articulated thoracolumbar spine and rib cage. *J. Biomech. Eng.* 137, 81003.
- Bruno, A.G., Cheng, B., Wang, W., Boussein, M.L., 2015b. Incorporating six degree-of-freedom intervertebral joint stiffness in a lumbar spine musculoskeletal model – method and performance in flexed postures. *J. Biomech. Eng.* 137, 1–9.
- Cholewicki, J., McGill, S.M., Norman, R.W., 1991. Lumbar spine loads during the lifting of extremely heavy weights. *Med. Sci. Sports Exerc.* 23, 1179–1186.
- Christophy, M., Faruk Senan, N.A., Lotz, J.C., O'Reilly, O.M., 2012. A musculoskeletal model for the lumbar spine. *Biomech. Model. Mechanobiol.* 11, 19–34.
- Crisco, J.J., Chen, X., Panjabi, M.M., Wolfe, S.W., 1994. Optimal marker placement for calculating the instantaneous center of rotation. *J. Biomech.* 27, 1183–1187.
- Daggfeldt, K., Thorstensson, A., 2003. The mechanics of back-extensor torque production about the lumbar spine. *J. Biomech.* 36, 815–825.
- De Zee, M., Hansen, L., Wong, C., Rasmussen, J., Simonsen, E.B., 2007. A generic detailed rigid-body lumbar spine model. *J. Biomech.* 40, 1219–1227.
- Delp, S.L., Anderson, F.C., Arnold, A.S., Loan, P., Habib, A., John, C.T., Guendelman, E., Thelen, D.G., 2007. OpenSim: open-source software to create and analyze dynamic simulations of movement. *IEEE Trans. Biomed. Eng.* 54, 1940–1950.
- Dooris, A.P., Goel, V.K., Grosland, N.M., Gilbertson, L.G., Wilder, D.G., 2001. Load-sharing between anterior and posterior elements in a lumbar motion segment implanted with an artificial disc. *Spine* 26, 122–129.
- Dreischarf, M., Schmidt, H., Putzier, M., Zander, T., 2015. Biomechanics of the L5–S1 motion segment after total disc replacement – influence of iatrogenic distraction, implant positioning and preoperative disc height on the range of motion and loading of facet joints. *J. Biomech.* 48, 3283–3291.
- Ellingson, A.M., Nuckley, D.J., 2015. Altered helical axis patterns of the lumbar spine indicate increased instability with disc degeneration. *J. Biomech.* 48, 361–369.
- Gertzbein, S.D., Holtby, R., Tile, M., Kapasouri, A., Chan, K.W., Cruickshank, B., 1984. Determination of a locus of instantaneous centers of rotation of the lumbar disc by moire fringes. A new technique. *Spine* 9, 409–413.
- Gertzbein, S.D., Seligman, J., Holtby, R., Chan, K.H., Kapasouri, A., Tile, M., Cruickshank, B., 1985. Centrode patterns and segmental instability in degenerative disc disease. *Spine* 10, 257–261.
- Gertzbein, S.D., Seligman, J., Holtby, R., Chan, K.W., Ogston, N., Kapasouri, A., Tile, M., 1986. Centrode characteristics of the lumbar spine as a function of segmental instability. *Clin. Orthop. Relat. Res.*, 48–51.
- Gracovetsky, S.A., Zeman, V., Carbone, A.R., 1987. Relationship between lordosis and the position of the centre of reaction of the spinal disc. *J. Biomed. Eng.* 9, 237–248.
- Han, K.-S., Kim, K., Park, W.M., Lim, D.S., Kim, Y.H., 2013a. Effect of centers of rotation on spinal loads and muscle forces in total disc replacement of lumbar spine. *Proc. Inst. Mech. Eng. H.* 227, 543–550.
- Han, K.-S., Rohlmann, A., Zander, T., Taylor, W.R., 2013b. Lumbar spinal loads vary with body height and weight. *Med. Eng. Phys.* 35, 969–977.
- Holzbaur, K.R.S., Murray, W.M., Delp, S.L., 2005. A model of the upper extremity for simulating musculoskeletal surgery and analyzing neuromuscular control. *Ann. Biomed. Eng.* 33, 829–840.
- Ignasiak, D., Dendorfer, S., Ferguson, S.J., 2015. Thoracolumbar spine model with articulated ribcage for the prediction of dynamic spinal loading. *J. Biomech.* 49, 959–966.
- McGill, S.M., 1997. The biomechanics of low back injury: Implications on current practice in industry and the clinic. *J. Biomech.* 30, 465–475.
- Ogston, N.G., King, G.J., Gertzbein, S.D., Tile, M., Kapasouri, A., Rubenstein, J.D., 1986. Centrode patterns in the lumbar spine: baseline studies in normal subjects. *Spine* 11, 591–595.
- Pearcy, M.J., Bogduk, N., 1988. Instantaneous axes of rotation of the lumbar intervertebral joints. *Spine* 13, 1033–1041.
- Pearsall, D.J., Reid, J.G., Livingston, L.A., 1996. Segmental inertial parameters of the human trunk as determined from computed tomography. *Ann. Biomed. Eng.* 24, 198–210.
- Schneider, G., Pearcy, M.J., Bogduk, N., 2005. Abnormal motion in spondylolytic spondylolisthesis. *Spine* 30, 1159–1164.
- Schultz, A., Andersson, G.B., Ortengren, R., Haderspeck, K., Nachemson, A., 1982. Loads on the lumbar spine. Validation of a biomechanical analysis by measurements of intradiscal pressures and myoelectric signals. *J. Bone Jt. Surg.*
- Senteler, M., Weisse, B., Rothenfluh, D.A., Farshad, M.T., Snedeker, J.G., 2017. Fusion angle affects intervertebral adjacent spinal segment joint forces-Model-based analysis of patient specific alignment. *J. Orthop. Res.* 35, 131–139.
- Senteler, M., Weisse, B., Rothenfluh, D.A., Snedeker, J.G., 2016. Intervertebral reaction force prediction using an enhanced assembly of OpenSim models. *Comput. Methods Biomech. Biomed. Eng.* 19, 538–548.
- Senteler, M., Weisse, B., Snedeker, J.G., Rothenfluh, D.A., 2014. Pelvic incidence–lumbar lordosis mismatch results in increased segmental joint loads in the unfused and fused lumbar spine. *Eur. Spine J.* 23, 1384–1393.
- Shan, G., Bohn, C., 2003. Anthropometrical data and coefficients of regression related to gender and race. *Appl. Ergon.* 34, 327–337.
- Sherman, M.A., Seth, A., Delp, S.L., 2013. What is a Moment Arm? Calculating Muscle Effectiveness in Biomechanical Models Using Generalized Coordinates. Volume 7B: 9th International Conference on Multibody Systems, Nonlinear Dynamics, and Control. ASME.

- Vasavada, A.N., Li, S., Delp, S.L., 1998. Influence of muscle morphometry and moment arms on the moment-generating capacity of human neck muscles. *Spine* 23, 412–422.
- Wong, K.W.N., Luk, K.D.K., Leong, J.C.Y., Wong, S.F., Wong, K.K.Y., 2006. Continuous dynamic spinal motion analysis. *Spine* 31, 414–419.
- Wu, M., Wang, S., Driscoll, S.J., Cha, T.D., Wood, K.B., Li, G., 2014. Dynamic motion characteristics of the lower lumbar spine: implication to lumbar pathology and surgical treatment. *Eur. Spine J.* 23, 2350–2358.
- Zander, T., Dreischarf, M., Schmidt, H., 2016. Sensitivity analysis of the position of the intervertebral centres of reaction in upright standing - a musculoskeletal model investigation of the lumbar spine. *Med. Eng. Phys.* 38, 297–301.
- Zander, T., Rohlmann, A., Bergmann, G., 2009. Influence of different artificial disc kinematics on spine biomechanics. *Clin. Biomech.* 24, 135–142.
- Zhu, R., Zander, T., Dreischarf, M., Duda, G.N., Rohlmann, A., Schmidt, H., 2013. Considerations when loading spinal finite element models with predicted muscle forces from inverse static analyses. *J. Biomech.* 46, 1376–1378.